

## On mixtures as working fluids of air-cooled ORC bottoming power plants of gas turbines

Krempus, Dabo; Bahamonde, Sebastian; van der Stelt, Teus P.; Klink, Wolfgang; Colonna, Piero; De Servi, Carlo M.

**DOI**

[10.1016/j.applthermaleng.2023.121730](https://doi.org/10.1016/j.applthermaleng.2023.121730)

**Publication date**

2024

**Document Version**

Final published version

**Published in**

Applied Thermal Engineering

**Citation (APA)**

Krempus, D., Bahamonde, S., van der Stelt, T. P., Klink, W., Colonna, P., & De Servi, C. M. (2024). On mixtures as working fluids of air-cooled ORC bottoming power plants of gas turbines. *Applied Thermal Engineering*, 236, Article 121730. <https://doi.org/10.1016/j.applthermaleng.2023.121730>

**Important note**

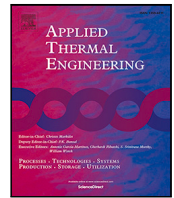
To cite this publication, please use the final published version (if applicable).  
Please check the document version above.

**Copyright**

Other than for strictly personal use, it is not permitted to download, forward or distribute the text or part of it, without the consent of the author(s) and/or copyright holder(s), unless the work is under an open content license such as Creative Commons.

**Takedown policy**

Please contact us and provide details if you believe this document breaches copyrights.  
We will remove access to the work immediately and investigate your claim.



# On mixtures as working fluids of air-cooled ORC bottoming power plants of gas turbines

Dabo Krempus<sup>a</sup>, Sebastian Bahamonde<sup>a</sup>, Teus P. van der Stelt<sup>b</sup>, Wolfgang Klink<sup>d</sup>,  
Piero Colonna<sup>a</sup>, Carlo M. De Servi<sup>a,c,\*</sup>

<sup>a</sup> Propulsion and Power, Delft University of Technology, Kluyverweg 1, 2629HS, Delft, The Netherlands

<sup>b</sup> Asimptote bv, Heeswijk-Dinther, The Netherlands

<sup>c</sup> Energy Technology Unit, VITO, Beretang 200, BE-2400, Mol, Belgium

<sup>d</sup> Siemens Energy AG, Erlangen, Germany

## ARTICLE INFO

### Keywords:

Organic Rankine cycle  
Waste heat recovery  
Binary mixtures

## ABSTRACT

The use of mixtures as working fluids of organic Rankine cycle (ORC) waste heat recovery (WHR) power plants has been proposed in the past to improve the matching between the temperature profile of the hot and the cold streams of condensers and evaporators, thus to possibly increase the energy conversion efficiency of the system. The goal of this study is to assess the benefits in terms of efficiency, environmental (GWP) and operational safety (flammability) that can be obtained by selecting optimal binary mixtures as working fluids of air-cooled ORC bottoming power plants of medium-capacity industrial gas turbines. Furthermore, two thermodynamic cycle configurations are analyzed, namely the simple recuperated cycle and the so-called split-cycle configurations. The benchmark case is a combined cycle power plant formed by an industrial gas turbine and an air-cooled recuperated ORC power unit with cyclopentane as the working fluid. The results of this study indicate that binary mixtures provide the designer with a wider choice of optimal working fluids, however, in the case of the recuperated-cycle configuration, no improvement in terms of combined cycle efficiency over the benchmark case can be achieved. The split-cycle configuration leads to an increase of combined cycle efficiency of the order of 1.5%, both in case of pure and blended working fluids. Furthermore, for this cycle configuration the use of Novec 649 as working fluid is advantageous because it is environmentally and operationally safe, and it does not involve any penalty in terms of combined cycle efficiency if compared to the benchmark case. Additionally, the use of this fluid would lead to a more compact turbine, as the corresponding thermodynamic cycle would determine a turbine volume flow ratio that is half of the value of the benchmark case and a specific enthalpy difference over the expansion that is one fifth.

## 1. Introduction

In the European Union alone, the amount of wasted thermal energy that could be recovered for further use is estimated to be about 300 TWh/year [1,2]. Bianchi et al. [1] report that 55% of this recoverable energy is due to heat sources with temperatures above 300 °C while the rest is available at lower temperatures. Papapetrou et al. [2] indicate similar values. A more recent report documents in more detail the availability of industrial waste heat in EU countries per industrial sector, temperature level and geographical location, further highlighting the large potential of this renewable-equivalent energy source [3].

High temperature industrial heat sources provide a substantial potential for waste heat recovery (WHR) and for waste-heat-to-power (WH2P) in particular. WH2P from high temperature thermal energy

and for large power capacities is traditionally realized by means of steam-cycle power plants, but the number of large high-temperature heat sources is very limited. For lower power capacities the resulting steam mass flow rate would be too small and the specific enthalpy over the expansion too large for the realization of efficient steam turbines [4]. The use of an organic compound as working fluid allows realizing simple and efficient turbines, and in general a simpler and more cost-effective power plant configuration. For example, the fluid can be chosen to keep the working fluid in the condenser at super-atmospheric pressure.

Recovering waste heat from stationary and mobile gas turbines, internal combustion and, in the future, fuel cell engines with ORC systems provides an enormous opportunity for efficiency increase and emission reduction. The most prominent limitation of using organic

\* Corresponding author at: Propulsion and Power, Delft University of Technology, Kluyverweg 1, 2629HS, Delft, The Netherlands.  
E-mail address: [c.m.deservi@tudelft.nl](mailto:c.m.deservi@tudelft.nl) (C.M. De Servi).

## Nomenclature

### Acronyms

Cond	condenser
GWP	global warming potential over 100 years
HRVG	heat recovery vapor generator
ODP	ozone depletion potential
Pre	preheater
Rec	recuperator
VLE	vapor liquid equilibrium

### Greek symbols

$\eta$	isentropic efficiency (–)
$\eta_{cc}$	combined cycle efficiency (–)
$\xi$	exergy loss (–)

### Subscripts

C	cold side fluid
crit	critical point
H	hot side fluid
in	inflowing
pp	pinch point

### Roman symbols

$\Delta h_{\text{turbine}}$	turbine enthalpy drop (kJ/kg)
$\dot{m}$	mass flow rate (kg/s)
$\dot{W}_{\text{fan}}$	air-cooler fan power demand (MW)
$\dot{W}_{\text{net}}$	ORC net power output (MW)
$T_{\text{limit}}$	thermal stability limit of fluid (K)
$T_{\text{NBP}}$	normal boiling point of fluid (K)
$z_i$	molar fraction (–)
p	pressure (Pa)
T	temperature (K)
VR	turbine volumetric flow ratio (–)

compounds as working fluids of high temperature ORC power plants is their relatively low thermal stability if compared, for instance, to that of water. The use of organic fluids featuring high thermal stability (some hydrocarbons, siloxanes, some phased-out refrigerants) is often restricted by regulations regarding operational safety (flammability) [5] and environmental sustainability (GWP, ODP) [6]. In this regard, the use of mixtures as working fluids may result in cycle configurations providing higher energy conversion efficiency [7] and, at the same time, compliance with regulatory requirements. Especially in the case of mobile applications and of power plants employing air-cooled condensers either because regulation forbids the use of water cooling or because they are located in remote and arid areas, the use of mixtures as working fluids may be advantageous. The efficiency of air-cooled ORC power plants might benefit from non-isothermal condensation because the power absorbed by fans, which may be rather large, can be reduced in comparison with the amount needed for the isothermal condensation of a pure working fluid. However, more heat transfer surface is usually required. In their work on mixtures as working fluids for air-cooled ORC WH2P systems for fuel cells, Angelino and Colonna [8,9] showed that the improved temperature profile matching in the condenser due to the working fluid temperature glide over condensation leads to a substantial reduction of air-cooler fan power at the cost of larger heat transfer surface, and may contribute to an increase of the combined cycle net power output. Moreover, the additional cost due to a larger condenser could be recovered in a very short time.

After the seminal works of Angelino and Colonna [8,9], researchers have investigated the use of mixtures as working fluids for various ORC applications such as waste heat recovery and conversion of solar and geothermal energy, see the literature reviews presented by Braimakis et al. [10] and Abadi and Kim [11]. While for low-temperature ORC power plants numerous studies indicate that the use of mixtures as working fluids allows for an increase of conversion efficiency, in case of high-temperature systems, contrasting results have been reported in the literature. Most of these works focus on water-cooled ORC systems as bottoming units of internal combustion engines (ICE). For instance, Fang et al. [12] considered as working fluids of a simple ORC system zeotropic mixtures composed by combining two high critical temperature hydrocarbons, namely decane and toluene, and two low critical temperature refrigerants, i.e., R245fa and R123. They found that the power output of the ORC bottoming unit operating with mixtures is always lower than that estimated in case toluene is the working fluid. However, the adoption of a 0.9 toluene / 0.1 decane mixture may allow for a lower levelized cost of electricity of the plant thanks to a reduction in the size of the heat exchangers that is achieved at the cost of a marginal decrease in power output with respect to the ORC operating with pure toluene. Conversely, in the case of heat recuperation from large Diesel engines for power generation on offshore platforms, Kolahi et al. [13] estimated significant gains in the efficiency of the ORC unit if mixtures of hexane and cyclohexane with the refrigerants R236ea and R245fa are adopted as working fluid. The improvement with respect to the efficiency achieved with the same pure fluids is up to 20%, while the corresponding reduction in the specific investment costs and payback time of the ORC unit is lower than 10%. Scaccabarozzi et al. [14] optimized the conceptual design of an ORC bottoming unit considering two ICE's as topping unit, featuring different exhaust gas temperatures, and two operating scenarios: in the first one, the output of the combined system consists only of electricity, while in the second one the plant is operated in cogeneration mode. The authors analyzed for each scenario more than twenty fluids and the binary mixtures resulting from their combination, if these mixtures feature a temperature glide over condensation of at least 5 °C. Their results show that mixtures allow for an ORC power output increase of the order of about 3% in all the considered scenarios. The authors attributed the limited efficiency improvement to the supercritical configuration of the optimal cycles: the temperature glide is exploited only over condensation and, as a result, the thermodynamic benefit of adopting mixtures in place of pure fluids is reduced. As an alternative to a supercritical cycle configuration, researchers have explored the adoption of mixtures in two cascaded ORC loops, see, e.g., [15,16]. These studies indicate that zeotropic mixtures allow for a higher ORC power output, though the extent of the increase varies significantly, from a few percentage points, as in [14], to up to 20%.

In case of solar power conversion, supercritical CO<sub>2</sub> power plants are one of the most promising solutions, because of their high conversion efficiency and the expected compactness of the equipment. Researchers have investigated the blending of CO<sub>2</sub> with other organic compounds featuring high thermal stability to improve further plant efficiency as well as to mitigate some of the technical challenges that supercritical CO<sub>2</sub> technology entails, e.g., the high pressure of the cycle [17–19]. Contrary to what observed for waste heat recovery from ICE, the researchers calculated substantial efficiency gains. With respect to the supercritical CO<sub>2</sub> power cycle, the relative increase in efficiency ranges from 5% to 15% depending on the considered minimum and maximum cycle temperature.

Regarding high-temperature WH2P systems (thermal source temperature above 300 °C), only Ren et al. [20] assessed the use of mixtures as working fluid of an ORC bottoming unit. The authors studied a gas turbine and water-cooled organic Rankine cycle combined system and included among the assessed working fluids mixtures of siloxanes, alkanes and aromatic hydrocarbons. Moreover, four commercial gas turbines with different exhaust temperatures (280–500 °C) and power

capacity (600 kW–53 MW) were considered as topping unit of the plant. Their results show that the mixtures may allow for marginal improvements of the ORC unit efficiency, except for small power capacity gas turbines, where they are outperformed by bottoming cycles using cyclopentane as working fluid.

Note that only a limited amount of fluids were considered in the majority of the cited literature, thus preventing the generalization of those results: better performance may be achieved with pure compounds or mixtures that were not considered. To address this limitation, Papadopoulos et al. [21] were the first to propose a Computer-Aided Molecular Design (CAMD) framework for the synthesis of binary mixtures suitable as working fluids of ORC power plants. Their methodology integrates an ORC system model with a group contribution method and a cubic equation of state to calculate the thermodynamic properties of the mixtures. Thanks to the group contribution method, it is possible to calculate with acceptable accuracy the thermodynamic properties of a fluid made by a generic molecule and then assess the corresponding performance through the ORC system model. This in turn enables the optimization of the molecular structure of the two working fluids based on the chosen objective functions. It follows that the ORC design is not limited by the chosen set of candidate fluids, provided that the group contribution method enables the modeling of a broad spectrum of fluids. In Ref. [21] the demonstrative academic case is a geothermal plant exploiting a brine at 95 °C. The objective functions are the maximization of the thermal and exergy efficiency as well as the minimization of the flammability characteristics of the two fluids. The resulting optimal working fluid is a blend of two fluorinated derivatives of propane. However, the authors did not compare the ORC power plant performance estimated in case of the optimal mixture working fluid with that of pure working fluids. This comparison is instead performed by Schilling et al. [22], who implemented a CAMD framework based on a group-contribution method applied to the physically-based perturbed-chain statistically associating fluid theory (PC-SAFT) equation of state, and capable of optimizing the thermo-economic performance of ORC processes operating with mixtures. The authors discovered that the potential of mixtures strongly depends on the temperature rise of the cooling water in the condenser and the temperature of the thermal source, and that the optimal mixture varies considerably with the considered process specifications. With regard to the effect of the thermal source temperature, the results of Schilling et al. [22] show that using binary mixtures as working fluids is very advantageous for low temperature heat sources in the range of 100–125 °C. The relative efficiency increase can be higher than 50%, while the reduction in the specific costs of the plant is much lower and of the order of 2–3%. For higher heat source temperatures, namely between 150–200 °C, the results of calculations do not provide any clear trend about the effect of using binary mixtures as working fluids on thermodynamic cycle efficiency. The net power output achieved with the optimal mixture is always 5–10% higher than the net power output obtained with the optimal pure component, confirming the potential of mixtures. At the same time, the economic benefit of adopting mixtures remains approximately independent from the thermal source inlet temperature.

It is therefore possible to conclude that the potential of mixtures as working fluids of ORC systems converting thermal sources at temperatures in excess of 300 °C has not been properly characterized yet. If, on the one hand, clear benefits have been demonstrated for supercritical CO<sub>2</sub> power cycles in solar applications, on the other, contradictory results are reported for other ORC systems, especially in case of waste heat recovery from ICE's. The reason may be the limited number of working fluids and mixtures considered by the researchers. Moreover, the studies investigating WH2P applications involving gas turbines or fuel cells are too few to draw a general conclusion. Another important limitation is that the majority of the literature about the use of zeotropic mixtures focuses on water-cooled ORC power plants despite the earlier works of Angelino and Colonna [8,9] already demonstrated

that the main advantage offered by fluid blends is the lower air-cooler fan power consumption enabled by the temperature glide over condensation. Moreover, water cooling is most often impossible either because of the typical geographical location of these power plants or because of the current regulatory framework.

This work contributes to the filling of the knowledge gap regarding the use of working fluid mixtures in high-temperature air-cooled ORC power plants for WH2P applications. The impact of using mixtures on combined cycle efficiency, especially considering its influence on fan power demand, the potential of selecting environmentally and operationally safe fluids, as well as the impact of the working fluid on turbine design were analyzed. A combined cycle power plant formed by an industrial gas turbine and an air-cooled recuperated ORC power unit with cyclopentane as the working fluid, a power plant that is similar to a product offered on the market, was chosen as the benchmark. Two different cycle configurations were analyzed and a very wide range of pure fluids (26) and binary mixtures (325) as the working fluid were considered. Optimal cycle parameters and working fluid combinations are subsequently identified using an evolutionary optimization algorithm targeting the net power output as the optimization objective. Given that there is no experimental database that could have supported the modeling of such an extensive set of blends, with compositions optimized for the considered application, the estimation of their thermodynamic properties requires a predictive equation of state (EoS) model. The chosen thermodynamic model is the PC-SAFT EoS [23], thanks to its capability to provide reasonably accurate values of mixture thermodynamic properties given a few pure component parameters.

## 2. Methodology

### 2.1. Thermodynamic cycle configurations

Two cycle configurations are considered in this study. With reference to Fig. 1, these are the recuperated cycle, and the novel *split-cycle* [24]. Both configurations assume the use of an air-cooled condenser (Cond). The main difference with respect to the common recuperated cycle is that, in the split-cycle, the flow is divided into two streams downstream of the pump. One stream passes through the recuperator (Rec) while the other one exchanges thermal energy with the heat source in the preheater (Pre). Both streams are merged before entering the heat recovery vapor generator (HRVG). The degree of mass flow that is split from the main stream ( $m_{frac}$ ) is defined as the fraction of mass flow rate through the recuperator cold side over that through the hot side.

The benchmark case is a combined-cycle power plant formed by a Siemens SGT-750 gas turbine and an ORC bottoming unit. This ORC system implements the recuperated-cycle configuration and uses cyclopentane as the working fluid. The gas turbine has a nominal power output  $\dot{W}_{GT}$  of 34.6 MW and a thermal efficiency  $\eta_{GT}$  of 38.5% at an ambient temperature  $T_{amb}$  of 30 °C. The net power output of the ORC system  $\dot{W}_{net}$  is 9.9 MW. This results in a combined cycle power output of 44.5 MW and a combined cycle efficiency  $\eta_{CC}$  of 49.5%, with  $\eta_{cc} = (\dot{W}_{GT} + \dot{W}_{net})/(\dot{W}_{GT}/\eta_{GT})$ .

### 2.2. Working fluids

The fluids selected for this analysis comprehend compounds featuring high thermal stability (HCs, PFCs, Siloxanes), low GWP and low flammability (HFC, HFOs, HCFOs). These are listed in Table 3 together with their main characteristics. The ozone depletion potential of all fluids except for HCFO-1244yd-Z and HCFO-1233zd-E is zero. For these two fluids, Arpagaus et al. [29] state ODP values of 1.2E–4 and 3.4E–4, respectively.

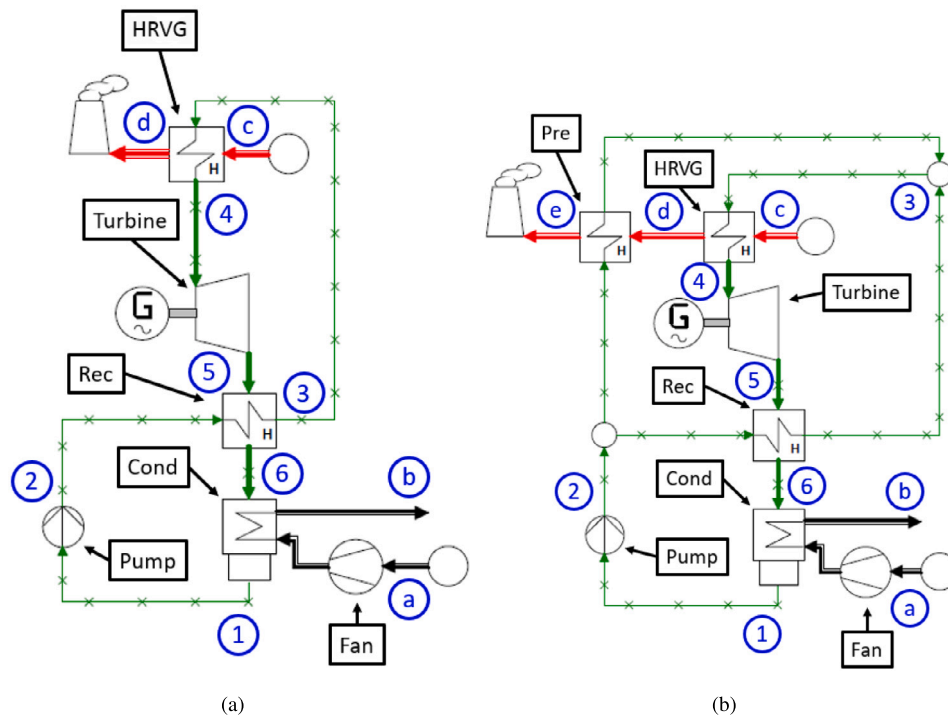


Fig. 1. Process flow diagrams of the recuperated-cycle (a) and split-cycle (b) configurations.

Table 1  
Thermodynamic cycle specifications.

Parameter	Value	Parameter	Value
$T_{HRVG_{H_{in}}}$ <sup>a</sup>	760.25 K	$\Delta T_{PP_{Rec}}$	10 K
$\dot{m}_{HRVG}$ <sup>a</sup>	105.6 kg/s	$\Delta p_{Rec_{H}}$	2500 Pa
$\Delta p_{HRVG_{H}}$	2500 Pa	$\Delta p_{Rec_{C}}$	2.5% of $p_{max}$
$\Delta p_{HRVG_{C}}$	2.5% of $p_{max}$	$\Delta p_{Pre}$ <sup>b</sup>	0 Pa
$\Delta T_{PP_{HRVG}}$	10 K	$\eta_{pump}$	70%
$\Delta T_{PP_{Cond}}$ <sup>a</sup>	7 K	$\eta_{turb}$	80%
$\Delta p_{cond_{H}}$	5000 Pa	$\eta_{fan}$	75%
$\Delta p_{cond_{C}}$	200 Pa	$T_{amb}$ <sup>a</sup>	303.15 K

<sup>a</sup> Values provided by Klink [25]. Remaining values are estimates.

<sup>b</sup> Entire pressure drop assumed in HRVG.

Table 2  
Simulation cases and settings.

Simulation case <sup>a</sup>	Design variables
pure/recuperated	$T_{min}, T_{max}, p_{max}$
pure/split	$T_{min}, T_{max}, p_{max}, m_{frac}$
binary/recuperated	$T_{min}, T_{max}, p_{max}, z_i$
binary/split	$T_{min}, T_{max}, p_{max}, z_i, m_{frac}$

<sup>a</sup> Working fluid composition/cycle configuration.

### 2.3. Thermodynamic models

Cycle calculations are performed by means of an in-house tool which relies on a widely adopted fluid property library [45] implementing a variety of models. Among these models, the PCP-SAFT equation of state is adopted in this study, see Ref. [23] for more details. Thanks to its predictive capabilities, the PCP-SAFT EoS is reasonably accurate also for the prediction of thermodynamic properties of mixtures, as showcased in the original papers documenting this thermodynamic model [23,46]. The accuracy of the PCP-SAFT model is confirmed by a recent study [47] aimed at developing a group contribution method for the prediction of its binary interaction parameters. The thermodynamic properties of binary mixtures formed by either two polar fluids or two

nonpolar fluids are generally predicted with high accuracy also if the binary interaction parameters  $k_{ij}$  are set equal to zero. However, a certain degree of uncertainty in the results can be expected for mixtures resulting from the combination of a polar and a nonpolar compound. The largest inaccuracy can be expected for mixtures formed by a polar and an associating fluid. None of the substances in Table 3 is formed by associating molecules. In light of these considerations and the fact that predictive methods for the binary interaction parameters of PCP-SAFT are still under development and are limited to hydrocarbons, all mixture binary interaction parameters are set to zero. This is common engineering practice in studies involving chemical processes if experimental data are unavailable for EoS calibration.

The air-cooler fan power consumption  $\dot{W}_{fan}$  is calculated as the product of the cooling air mass flow rate  $\dot{m}_{cond_C}$  times the condenser cold-side pressure drop  $\Delta p_{cond_C}$  divided by air density and fan isentropic efficiency. For the same amount of rejected thermal power, a temperature glide over condensation allows for an increased heating of the cooling air and thus a reduction in  $\dot{m}_{cond_C}$ . As  $\Delta p_{cond_C}$  is fixed (see in Table 1), only the impact of the  $\dot{m}_{cond_C}$  variation on  $\dot{W}_{fan}$  is accounted for in this analysis. The gas turbine exhaust gas is modeled as an ideal gas mixture with a molar composition of 73.9% N<sub>2</sub>, 13.8% O<sub>2</sub>, 3.1% CO<sub>2</sub>, 8.1% H<sub>2</sub>O and 0.9% Ar [25]. Table 1 lists the overall cycle specifications.

### 2.4. Optimization problem

Numerical optimization is used to identify a cycle design that maximizes net power output of the ORC unit ( $\dot{W}_{net}$ ). Therefore, the following constrained single-objective optimization problem is solved:

$$\begin{aligned} & \text{maximize} && F(x) = \dot{W}_{net}, \\ & \text{subject to} && p_{min} \geq 1.013 \text{ bar}, \\ & && x_i^L \leq x_i \leq x_i^U. \end{aligned} \quad (1)$$

The optimization problem comprises one constraint that ensures a super-atmospheric condensing pressure. This constraint is adopted in agreement with the usual conservatism that informs design choices



**Table 3**  
List of candidate fluids.

	Synonym	Chemical formula	CAS-Nr.	$p_{crit}$ ( $10^5$ Pa)	$T_{crit}$ (K)	Molecular weight (kg/kmol)	$T_{limit}$ (K)	$T_{NBP}$ (K)	GWP	Flammability
Old Refrig.	R125	C2HF5	354-33-6	36.2 <sup>a</sup>	339.2 <sup>a</sup>	120.0 <sup>a</sup>	669 <sup>b</sup>	225 <sup>a</sup>	3500 <sup>c</sup>	No <sup>c</sup>
	R134a	C2H2F4	811-97-2	40.6 <sup>a</sup>	374.2 <sup>a</sup>	102.0 <sup>a</sup>	641 <sup>b</sup>	247 <sup>a</sup>	1300 <sup>d</sup>	No <sup>d</sup>
	R32	CH2F2	75-10-5	57.8 <sup>a</sup>	351.3 <sup>a</sup>	52.0 <sup>a</sup>	843 <sup>c</sup>	221 <sup>a</sup>	675 <sup>c</sup>	Mild <sup>c</sup>
	R245fa	C3H3F5	460-73-1	36.4 <sup>a</sup>	427.2 <sup>a</sup>	134.0 <sup>a</sup>	573 <sup>s</sup>	288 <sup>a</sup>	858 <sup>f</sup>	No <sup>d</sup>
Modern Refrig.	HFO-1336mzz-Z	C4H2F6	692-49-9	30.5 <sup>d</sup>	444.30 <sup>d</sup>	164.1 <sup>d</sup>	523 <sup>e</sup>	306 <sup>d</sup>	2 <sup>d</sup>	No <sup>d</sup>
	HFO-1336mzz-E	C4H2F6	66711-86-2	32.9 <sup>d</sup>	412.5 <sup>d</sup>	164.1 <sup>d</sup>	523 <sup>g</sup>	281 <sup>d</sup>	18 <sup>d</sup>	No <sup>d</sup>
	HCFO-1224yd-Z	C3HClF4	111512-60-8	33.8 <sup>d</sup>	429.2 <sup>d</sup>	148.5 <sup>d</sup>	448 <sup>f,t,j</sup>	287 <sup>d</sup>	1 <sup>d</sup>	No <sup>d</sup>
	HCFO-1233zd-E	C3H2ClF3	102687-65-0	36.2 <sup>d</sup>	439.7 <sup>d</sup>	130.5 <sup>d</sup>	450 <sup>k,t</sup>	291 <sup>d</sup>	7 <sup>k</sup>	No <sup>d</sup>
	HFO-1234yf	C3H2F4	754-12-1	33.8 <sup>a</sup>	367.9 <sup>a</sup>	114.0 <sup>a</sup>	N/A <sup>t</sup>	244 <sup>a</sup>	4 <sup>h</sup>	Mild <sup>j</sup>
	HFO-1243zf	C3H3F3	677-21-4	36.1 <sup>a</sup>	378.6 <sup>a</sup>	96.1 <sup>a</sup>	N/A <sup>t</sup>	248 <sup>a</sup>	0.8 <sup>h</sup>	Mild <sup>j</sup>
	Novec 649	C6F12O	756-13-8	18.7 <sup>a</sup>	441.8 <sup>n</sup>	316.0 <sup>i</sup>	573 <sup>i</sup>	322 <sup>i</sup>	1 <sup>i</sup>	No <sup>j</sup>
HCs	cyclopentane	C5H10	287-92-3	45.1 <sup>a</sup>	511.7 <sup>a</sup>	70.1 <sup>a</sup>	573 <sup>c</sup>	322 <sup>a</sup>	6 <sup>c</sup>	Yes <sup>c</sup>
	toluene	C7H8	108-88-3	41.1 <sup>a</sup>	591.8 <sup>a</sup>	92.1 <sup>a</sup>	673 <sup>c</sup>	384 <sup>a</sup>	3.3 <sup>o</sup>	Yes <sup>c</sup>
	isobutane	C4H10	75-28-5	36.4 <sup>a</sup>	407.8 <sup>a</sup>	58.1 <sup>a</sup>	593 <sup>q</sup>	261 <sup>a</sup>	3 <sup>d</sup>	Yes <sup>d</sup>
	propane	C3H8	74-98-6	42.5 <sup>a</sup>	369.8 <sup>a</sup>	44.1 <sup>a</sup>	633 <sup>r</sup>	231 <sup>a</sup>	3 <sup>d,o</sup>	Yes <sup>d</sup>
	ethane	C2H6	74-84-0	48.7 <sup>a</sup>	305.3 <sup>a</sup>	30.1 <sup>a</sup>	633 <sup>r</sup>	185 <sup>a</sup>	2.9 <sup>o</sup>	Yes
Siloxanes	D4	C8H24O4Si4	556-67-2	13.2 <sup>a</sup>	586.5 <sup>a</sup>	296.6 <sup>a</sup>	623 <sup>c</sup>	448 <sup>a</sup>	0 <sup>c</sup>	Mild <sup>c</sup>
	D5	C10H30O5Si5	541-02-6	10.4 <sup>a</sup>	617.4 <sup>a</sup>	370.8 <sup>a</sup>	623 <sup>c</sup>	484 <sup>a</sup>	0 <sup>c</sup>	Mild <sup>c</sup>
	D6	C12H36O6Si6	540-97-6	9.01 <sup>a</sup>	645.8 <sup>a</sup>	444.9 <sup>a</sup>	623 <sup>c</sup>	518 <sup>a</sup>	0 <sup>c</sup>	Mild <sup>c</sup>
	MM	C6H18OSi2	107-46-0	19.2 <sup>a</sup>	519.0 <sup>a</sup>	162.4 <sup>a</sup>	573 <sup>c</sup>	374 <sup>a</sup>	0 <sup>c</sup>	Yes <sup>c</sup>
	MDM	C8H24O2Si3	107-51-7	14.6 <sup>a</sup>	564.4 <sup>a</sup>	236.5 <sup>a</sup>	573 <sup>c</sup>	426 <sup>a</sup>	0 <sup>c</sup>	Mild <sup>c</sup>
	MD2M	C10H30O3Si4	141-62-8	11.9 <sup>a</sup>	599.4 <sup>a</sup>	310.7 <sup>a</sup>	573 <sup>c</sup>	477 <sup>a</sup>	0 <sup>c</sup>	Mild <sup>c</sup>
	MD3M	C12H36O4Si5	141-63-9	9.45 <sup>a</sup>	628.4 <sup>a</sup>	384.8 <sup>a</sup>	573 <sup>c</sup>	503 <sup>a</sup>	0 <sup>c</sup>	Mild <sup>c</sup>
MD4M	C14H42O5Si6	107-52-8	8.04 <sup>a</sup>	653.2 <sup>a</sup>	459.0 <sup>a</sup>	573 <sup>c</sup>	533 <sup>a</sup>	0 <sup>c</sup>	Mild <sup>c</sup>	
PFCs	PP2	C7F14	355-02-2	20.2 <sup>m</sup>	486.4 <sup>m</sup>	350.1 <sup>m</sup>	673 <sup>l</sup>	349 <sup>m</sup>	N/A <sup>u</sup>	No <sup>l</sup>
	PP5	C10F18	306-94-5	17.8 <sup>m</sup>	565.1 <sup>m</sup>	462.1 <sup>m</sup>	673 <sup>l</sup>	415 <sup>m</sup>	7190 <sup>p</sup>	No <sup>l</sup>

<sup>a</sup>Rowley et al. [26] using 2019 Database.

<sup>b</sup>Calderazzi and Colonna [27].

<sup>c</sup>Astolfi and Macchi [28].

<sup>d</sup>Arpagaus et al. [29].

<sup>e</sup>Kontomaris [30].

<sup>f</sup>Mateu-Royo et al. [31].

<sup>g</sup>Juhasz [32].

<sup>h</sup>McLinden et al. [33].

<sup>i</sup>3M Corporation [34].

<sup>j</sup>Takizawa et al. [35].

<sup>k</sup>Perkins et al. [36].

<sup>l</sup>F2 Chemicals Ltd. [37].

<sup>m</sup>Marsh et al. [38].

<sup>n</sup>McLinden et al. [39].

<sup>o</sup>Collins et al. [40].

<sup>p</sup>IPCC [41].

<sup>q</sup>Dai et al. [42].

<sup>r</sup>Acc. to Preisfänger and Brüggemann [43]

the compound is present as decomposition

product of MM at  $T > 633.15$  K.

<sup>s</sup>Angelino and Invernizzi [44].

<sup>t</sup>For this analysis 523 K was assumed.

<sup>u</sup>Assumed to be same as for PP5.

related to real-world power plants so as to ensure technical and economic feasibility. If the pressure in the condenser is greater than the atmospheric pressure, ambient air cannot leak into the system. Avoiding inward air leakage provides two operational advantages: first, in case the working fluid is flammable, leaked air can lead to the formation of an ignitable mixture inside the system which poses a safety issue; second, oxygen is a catalyst for thermal decomposition of the working fluid which reduces fluid lifetime and decreases the plant performance. In case of a configuration with sub-atmospheric condenser, it is therefore necessary to adopt a vacuum system, which introduces additional cost and may affect the reliability of the plant.

Depending on the simulation case, the design vector  $x$  consists of up to five variables. Table 4 lists the single design variables  $x_i$  considered in the optimization together with their lower bounds  $x^L$  and upper bounds  $x^U$ . In case of mixture working fluids, there are no predictive methods to determine the thermal stability limit given the characteristics of the molecules in the blend or the thermal stability limit of the pure constituents. In addition, experimental studies are very limited and show contradictory results. Liu et al. [48] investigated the thermal stability of a mixture of two refrigerants, R32 and R1234ze(E). The experimental data show that the thermal stability limit of the mixture is equal to that of the fluid that decomposes at the lowest temperature, R1234ze(E). The mixing of the two refrigerants promotes also the pyrolysis of R32 at a temperature that is lower than the decomposition temperature of the fluid if unmixed. A more complex interaction was instead observed by Gallarini et al. [49] for the mixture of two siloxanes, MM and MDM, whereby a recombination of the two molecules seems to enhance the thermal stability of MDM, the less thermally stable compound in the mixture. Due to the lack of experimental information and a general theory of thermal degradation of mixtures, in this study the upper bound of  $T_{max}$  is conservatively set

**Table 4**

Design variables and their respective bounds.

Variables ( $x_i$ )	Description (Unit)	Bounds ( $x^L/x^U$ )
$T_{min}$	Minimum temperature ORC working fluid (K)	281/303
$T_{max}$	Maximum temperature ORC working fluid (K)	473/ $\min(T_{limit,A}, T_{limit,B})$
$p_{r,max}$	Maximum reduced pressure ORC working fluid (-)	0.8/1.2
$m_{frac}$	Split cycle mass flow fraction (-)	0.1/0.9
$z_i$	Mixture molar composition (-)	0.0/1.0

equal to the lowest thermal stability limit of the involved compounds  $T_{limit,A}$  and  $T_{limit,B}$ , respectively. In case of pure fluids,  $T_{max}$  is set equal to the thermal stability limit reported in Table 3. The upper bound of the maximum reduced pressure  $p_{max,r} = p_{max}/p_{crit}$  is set to 1.2. Higher cycle pressures offer limited benefits in terms of cycle efficiency due to the increased pump power demand. High pump power demand also leads to an increased sensitivity of cycle efficiency to pump isentropic efficiency. Consequently, higher cycle pressure leads to increased component complexity and cost. For example, as opposed to the off-the-shelf pumps commonly used for subcritical ORC systems, a multi-stage pump may be required for supercritical-cycle power plants. Furthermore, the primary heat exchanger walls need to be thicker to sustain higher pressure [28]. The optimization problem is solved using the genetic algorithm eaMuPlusLambda implemented in the DEAP Python library [50].

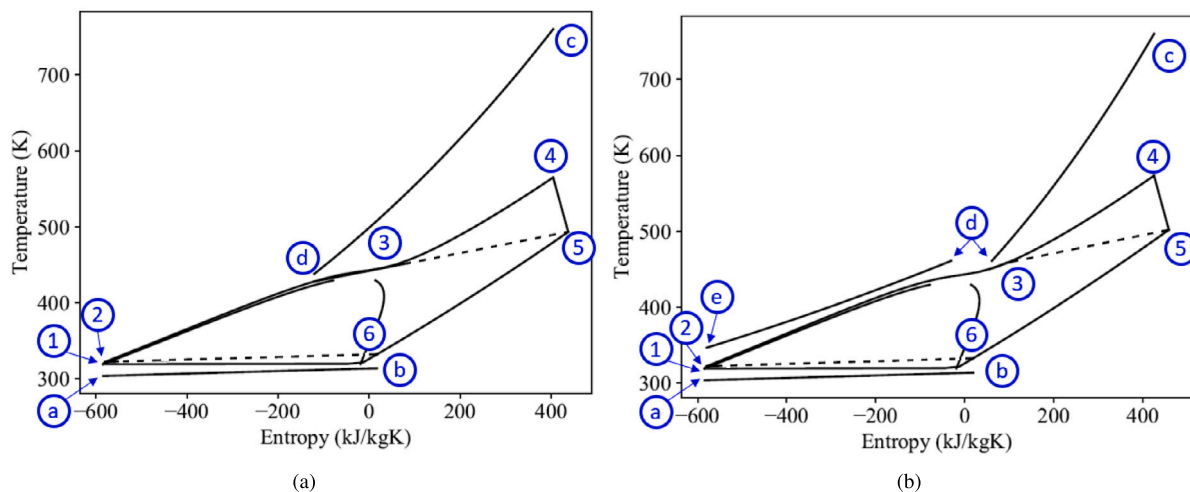


Fig. 2.  $Ts$ -diagram representation of the processed forming the recuperated-cycle (a) and split-cycle (b) configurations in case R245fa is the working fluid; The thermodynamic state numbering is consistent with that of Fig. 1.

Note 1: dashed lines indicate heat transfer between hot and cold recuperator streams; Note 2: the gap in saturation curve close to the critical point is due to convergence problems of the vapor–liquid equilibrium calculation very close to the critical point.

### 3. Results

325 binary mixtures resulting from the combination of the fluids in Table 3 are considered as the working fluid of the bottoming ORC unit. Not all the combinations of working fluids could be assessed because in some cases the thermodynamic property calculations fail and in other cases no condensation occurs for the considered range of minimum cycle pressures. The performance of cycles employing binary mixtures is compared against that achievable with cycles employing pure working fluids. All simulations are run based on the cycle specifications listed in Table 1 and the optimization settings given in Tables 2 and 4. Only cases that fulfill the constraint of super-atmospheric condensing pressure are presented hereafter. Fig. 2 shows a comparison between the processes of the recuperated-cycle and of the split-cycle configurations in the temperature entropy diagram of R245fa as an example. Both cycles are supercritical and feature a similar minimum and maximum temperature. The maximum temperatures are close to the estimated thermal stability limit of the working fluid, which is 573 K. The split-cycle allows to recover substantially more thermal energy from the exhaust gases due to the preheater. The relative increase in combined cycle efficiency is about 3%. However, such a performance increase is not obtained for all fluids and depends on the fluid critical temperature  $T_{crit}$  as discussed in Section 4.

Fig. 3 presents  $\dot{W}_{net}$  as a function of  $T_{crit}$  and molecular complexity for the recuperated-cycle and split-cycle configurations. According to Angelino et al. [51] the molecular complexity of the working fluid is “a function of the number and mass of the atoms forming the molecule and controls the shape of the saturation curve in the  $T$ - $S$  (sic) plane”. A positive value of the molecular complexity parameter  $\sigma$  is therefore associated with a larger value of the isobaric specific heat, a smaller value of the latent heat of vaporization, and a positive slope of the vapor saturation curve in the temperature-entropy diagram. Likewise, negative values of the molecular complexity are associated to a lower complexity of the molecules, larger values of the latent heat of vaporization and a negative slope of the vapor saturation curve in the temperature-entropy diagram. Note that the  $T_{crit}$  values are calculated as prescribed by the PCP-SAFT model and therefore might differ from experimental values. Higher power output can be achieved with the split-cycle configuration as compared to the recuperated-cycle configuration. Furthermore, with the split-cycle configuration, the best performance is obtained with fluids with lower  $T_{crit}$ .

Fig. 4 presents values of  $\eta_{cc}$  in relation to a representative selection of fluids. The corresponding working fluid composition is indicated

in Table 3. Non-flammable fluids with a GWP  $\leq 150$  are highlighted in blue in Fig. 4. The results show that the split-cycle configuration leads to a better performance with all the considered working fluids and can also outperform the benchmark cycle. Furthermore, some low GWP/non-flammable fluids allow to achieve a performance comparable to that of the benchmark, if the split-cycle configuration is adopted. In the case of the recuperated-cycle configuration with a pure working fluid, cyclopentane is the optimal working fluid, while, in the case of the split-cycle configuration, R245fa is the optimal working fluid, followed by isobutane and cyclopentane. Mixtures provide a wider range of fluids whose use offer a good combined cycle performance, but, as is the case for the recuperated-cycle configuration, the benchmark provides the best performance. Only in the case of the split-cycle configuration, the use of a mixture working fluid is beneficial if compared to a pure fluid, including cyclopentane. Despite the large variety of considered mixtures, in case of the recuperated-cycle configuration, 19 of the 20 mixtures providing the best  $\eta_{cc}$  contain cyclopentane with a mole fraction above 90%. Furthermore, among the 100 mixtures providing the best  $\eta_{cc}$ , 10 feature a low GWP and are non-flammable in the case of the recuperated-cycle configuration and 13 in the case of the split-cycle configuration.

### 4. Discussion

#### 4.1. Relation between cycle configuration and fluid critical temperature

Fig. 5 shows  $\eta_{cc}$  with respect to  $T_{crit}$  for both the recuperated-cycle and split-cycle configurations. In case of the split-cycle configuration,  $\eta_{cc}$  reaches the highest values for values of  $T_{crit}$  that are approximately 100 K lower than the  $T_{crit}$  of the fluids providing the best performance in case of the recuperated-cycle configuration. The reason is that the amount of thermal energy recovery associated with the split-cycle configuration does not decrease with the adoption of high degree of recuperation that fluids with lower critical temperature require to achieve high conversion efficiency.

#### 4.2. Effect of temperature glide

The isobaric phase change of a zeotropic mixture is non-isothermal, therefore it occurs with a temperature glide. This physical behavior is beneficial for the matching of the temperature profiles of the working fluid and air in the condenser and of the working fluid and exhaust

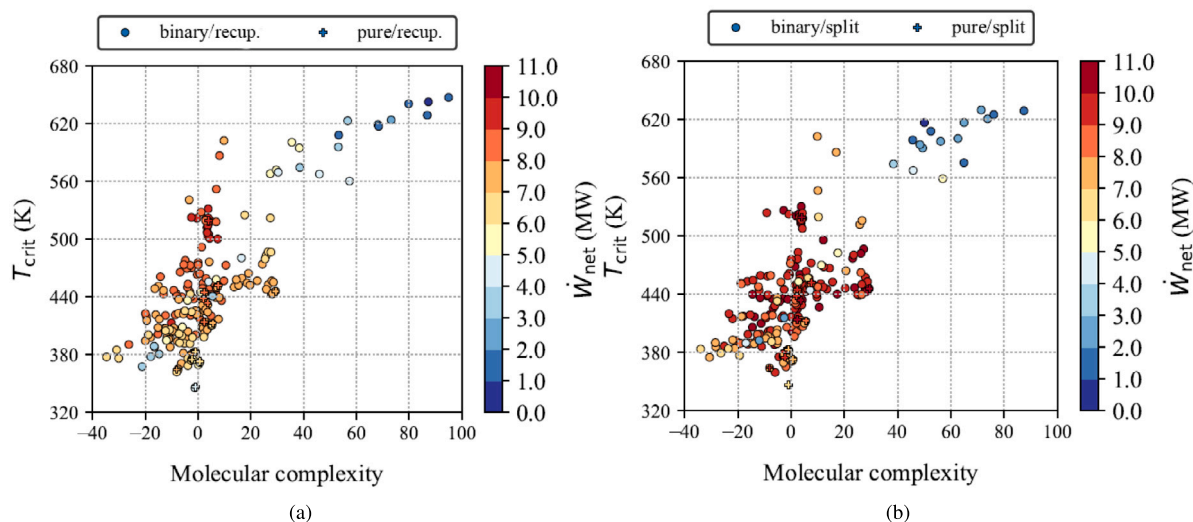


Fig. 3.  $\dot{W}_{\text{net}}$  as a function of  $T_{\text{crit}}$  and molecular complexity for both the recuperated-cycle (a) and the split-cycle (b) configurations.

Table 5

Table of selected fluids.

Fluid	pure/recuperated	pure/split	binary/recuperated	binary/split
1	cyclopentane	R245fa	cyclopentane[0.92]& R134a[0.08]	R245fa[0.72]& PP2[0.28]
2	HFO-1233zd-Z <sup>a</sup>	isobutane	cyclopentane[0.79]& R245fa[0.21]	R245fa[0.68]& cyclopentane[0.32]
3	R245fa	cyclopentane	cyclopentane[0.80]& HFO-1336mzz-Z[0.20]	cyclopentane[0.93]& isobutane[0.07]
4	HFO-1336mzz-Z <sup>a</sup>	Novec 649 <sup>a</sup>	R245fa[0.94]& D5[0.06]	Novec 649[0.95]& R134a[0.05]*
5	HCFO-1224yd-Z <sup>a</sup>	HFO-1336mzz-Z <sup>a</sup>	HCFO-1233zd-E[0.83]& toluene[0.17]	R32[0.83]& toluene[0.17]
6	isobutane	R134a	HCFO-1224yd-Z[0.90]& MM[0.10]	HFO-1336mzz-Z[0.92]& HFO-1243zf[0.08]
7	R32	HCFO-1224yd-Z <sup>a</sup>	isobutane[0.73]& R32[0.27]	propane[0.89]& D4[0.11]
8	Novec 649 <sup>a</sup>	R32	HCFO-1233zd-E[0.61]& HFO-1336mzz-Z[0.39] <sup>a</sup>	Novec 649[0.85]& MM[0.15]
9	HFO-1336mzz-E <sup>a</sup>	HCFO-1233zd-Z <sup>a</sup>	isobutane[0.80]&Novec 649[0.20]	HCFO-1233zd-E[0.78]& R134a[0.22]
10	R134a	HFO-1336mzz-E <sup>a</sup>	HCFO-1224yd-Z[0.94]& HFO-1243zf[0.06]	HCFO-1224yd-Z[0.76]& isobutane[0.24]

<sup>a</sup> Fluids with GWP  $\leq 150$  and zero flammability.

Note: numbers in brackets indicate molar composition  $z_i$ .

gas in the evaporator. Since most optimum cycle configurations considered in this analysis are of the supercritical type, evaporation is not affected by the temperature glide. However, the temperature glide in the condenser can decrease the fan power demand  $\dot{W}_{\text{fan}}$  of air-cooled ORC systems, which in turn can yield to an increase of  $\dot{W}_{\text{net}}$ .

Fig. 6 shows  $\dot{W}_{\text{net}}$  as a function of  $\dot{W}_{\text{fan}}$  and condenser temperature glide occurring across the vapor–liquid equilibrium (VLE) region  $\Delta T_{\text{condH-VLE}}$  for the recuperated cycle configuration.  $\dot{W}_{\text{fan}}$  reduces for increasing values of the  $\Delta T_{\text{condH-VLE}}$ . High values of  $\dot{W}_{\text{net}}$  are however only obtained for a narrow range of low  $\Delta T_{\text{condH-VLE}}$  values. Outside this range the beneficial  $\dot{W}_{\text{fan}}$  reduction is offset by the decrease in thermodynamic efficiency. Fig. 7 shows  $\Delta T_{\text{condH-VLE}}$  for the selected fluids listed in Table 5.

The question remains, why  $\dot{W}_{\text{net}}$  does not benefit from the reduction of  $\dot{W}_{\text{fan}}$  with increasing temperature glide. To answer this question an exergy analysis was performed. For the recuperated-cycle configuration, Fig. 8 provides a comparison between exergy losses in case cyclopentane is the working fluid with the losses in case binary mixtures are the working fluid, according to Table 5. While a slight trend

towards reduced condenser losses can be observed for the mixtures, the use of mixtures leads to an overall increase in exergy losses associated with the heat transfer in the HRVG or, in a few cases, in the recuperator. Furthermore,  $\dot{W}_{\text{fan}}$  contributes little to the losses. Therefore, for the specific application investigated in this study, a reduction of  $\dot{W}_{\text{fan}}$ , e.g., due to the temperature glide, only has a small impact on the plant overall performance.

#### 4.3. Impact of condensation pressure on cycle performance

Based on the following reasoning, it is hypothesized that lifting the super-atmospheric condensation pressure constraint might lead to a better performance of cycle configurations using mixtures as working fluids. A relaxation of this constraint would allow lower condensation temperatures. Lower condensation temperatures in turn would result in a lower condenser cold-side temperature difference and consequently to a higher  $\dot{m}_{\text{fan}}$  demand for a given condenser heat load. In the assumption that the condenser is designed for similar air speed, an increase



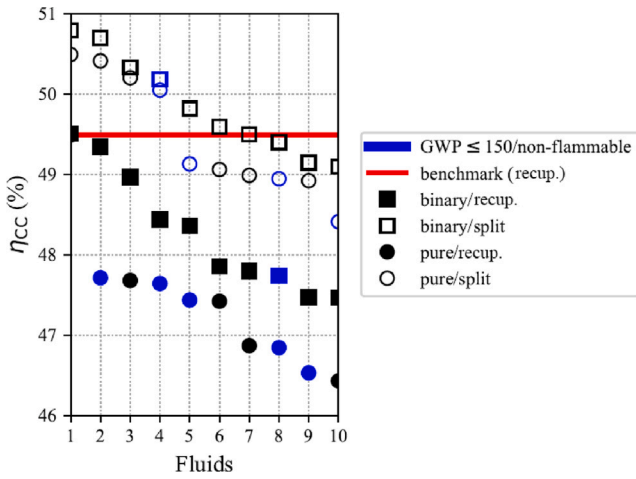


Fig. 4.  $\eta_{cc}$  corresponding to a selection of working fluids. The fluid number identifier is listed in Table 5.

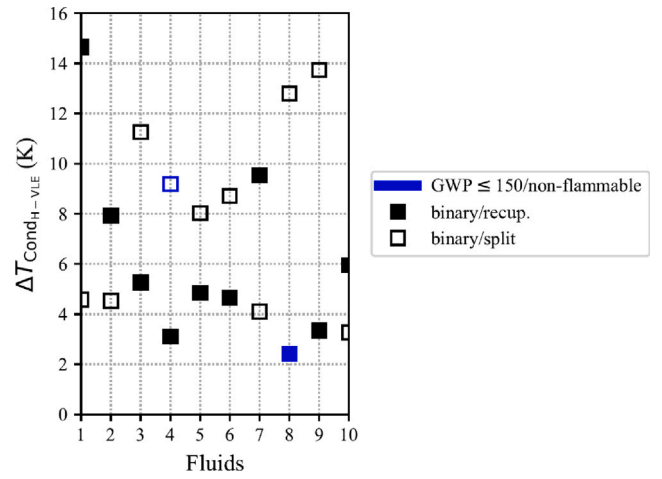


Fig. 7.  $\Delta T_{\text{Cond}_{H-VLE}}$  for selected fluids. Fluid number identifier in Table 5.

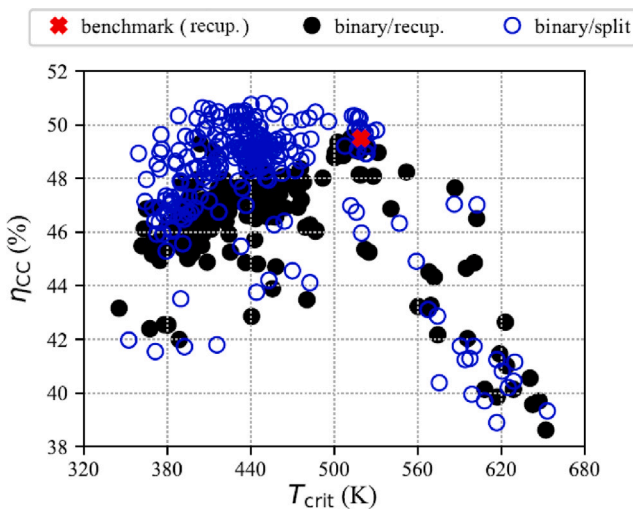


Fig. 5. Comparison of  $\eta_{cc}$  over  $T_{crit}$ .

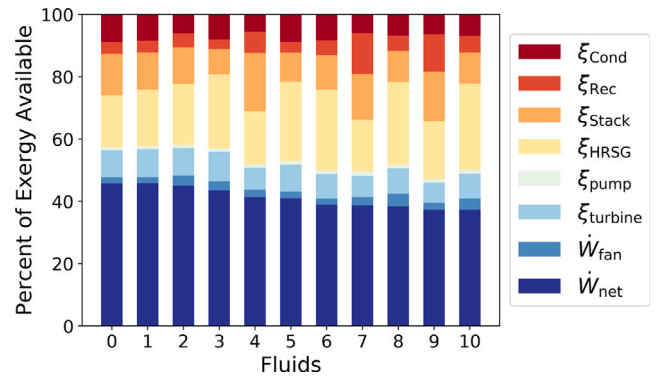


Fig. 8. Exergy analysis comparing the recuperated-cycle configuration using the benchmark working fluid cyclopentane (Fluid 0) with the binary/recuperated cases according to Table 5 indicated with their respective fluid number. Note: Exergy available assumes cooling of the heat source to ambient conditions, therefore,  $\xi_{\text{Stack}}$  represents the lost exergy at the HRVG exit.

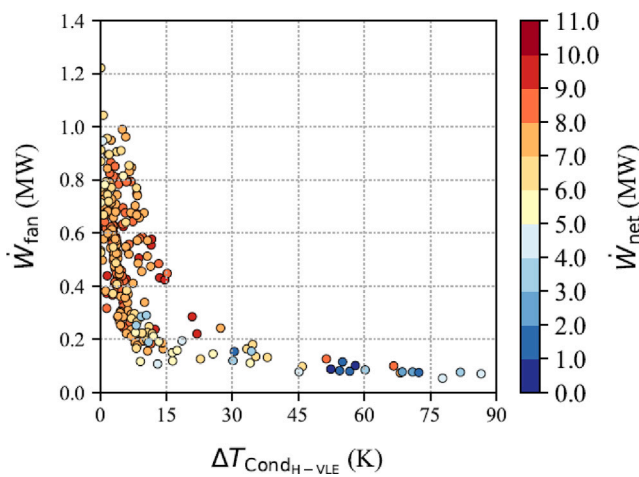


Fig. 6.  $\dot{W}_{net}$  as a function of  $\dot{W}_{fan}$  and  $\Delta T_{\text{Cond}_{H-VLE}}$  for the binary/recuperated case.

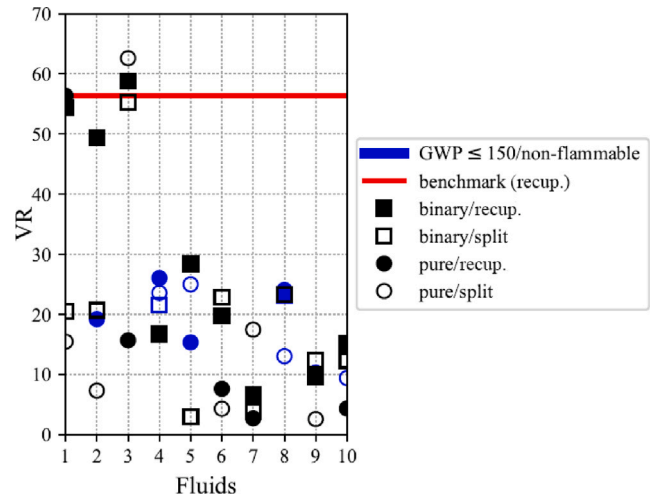


Fig. 9.  $VR$  for selected fluids. Fluid number identifier in Table 5.

in  $\dot{m}_{fan}$  would result in an increase of  $\dot{W}_{fan}$ . In this case, a temperature glide of the working fluid may therefore be more beneficial, in that it increases the temperature difference of the cooling air across the condenser.

In order to verify this hypothesis, all pure/recuperated and binary/recuperated simulations are re-run without imposing the super-atmospheric condensation pressure constraint. From the analysis of the results the following observations can be made. First of all, lifting the

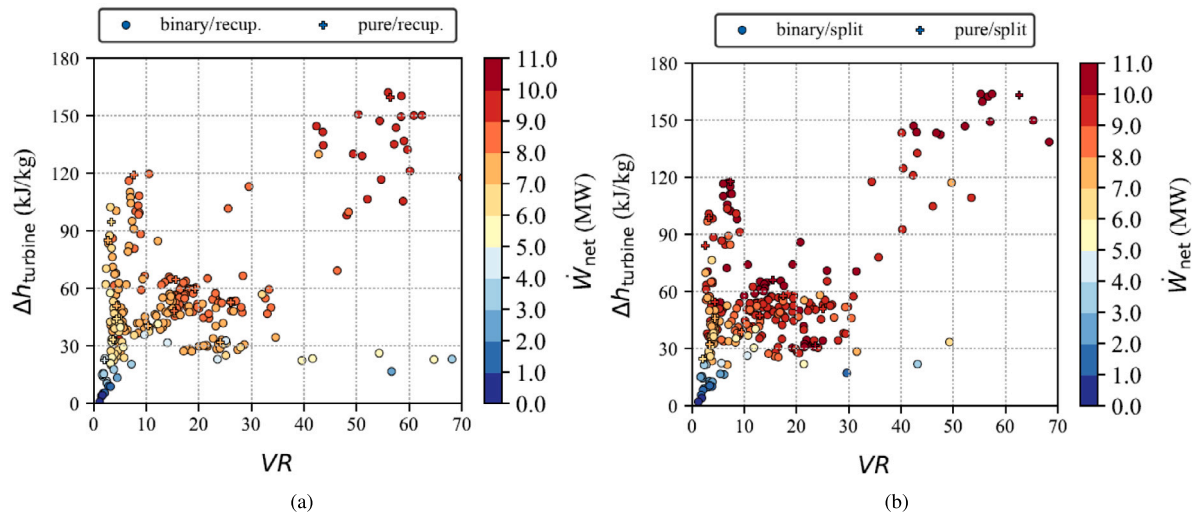


Fig. 10.  $\dot{W}_{\text{net}}$  as a function of  $\Delta h_{\text{turbine}}$  and  $VR$  for the recuperated-cycle (a) and split-cycle (b).

pressure constraint results in an increased range of feasible solutions including cycles using pure toluene and siloxanes as working fluids and cycles using mixtures containing toluene and siloxanes with large mole fractions. Secondly, for the cycles employing pure working fluids it is observed that the condenser cold-side temperature difference is smaller, which results in larger  $\dot{W}_{\text{fan}}$ . If toluene is the working fluid, the cycle efficiency is the maximum among all considered cases. However the calculated efficiency is very similar to that calculated in case cyclopentane is the working fluid. In both cases, the computed  $\dot{W}_{\text{net}}$  is slightly above 10 MW. Thirdly, the cycles employing binary mixtures as working fluid do not result in improved  $\eta_{\text{cc}}$ . Again, the efficiency of cycles with mixtures based on toluene as working fluid is slightly better than that of cycles with cyclopentane-based mixtures. However, the  $\Delta h_{\text{turbine}}$  and  $VR$  (around 500) associated with toluene are larger if compared to those associated with cyclopentane. The impact of these parameters on turbine design is discussed in Section 4.4. Therefore, the hypotheses put forward that cycle performance may benefit from the adoption of working fluid mixtures in case of lower condensation pressures is invalid for the considered application.

#### 4.4. Working fluid and turbine design

Turbine design complexity, size, efficiency and therefore cost, are driven by the specific enthalpy difference  $\Delta h_{\text{turbine}}$  and the volume flow ratio  $VR$  of the working fluid vapor over the expansion [28]. Fig. 10 displays the variation of these parameters for pure fluids and binary mixtures. With the recuperated-cycle configuration, the highest  $\eta_{\text{cc}}$  is achieved with fluids featuring high  $\Delta h_{\text{turbine}}$  and  $VR$ . These fluids contain a large mole fraction of cyclopentane. On the other hand, with the split-cycle, high  $\eta_{\text{cc}}$  is obtained with fluids also featuring lower  $\Delta h_{\text{turbine}}$  and  $VR$ . For example, Fig. 10 (b) indicates that high performance can be attained with fluids leading to a  $VR$  range from 10 to 25 and a  $\Delta h_{\text{turbine}}$  between 30 and 60 kJ/kg. Comparing this  $VR$  range with the data given in Fig. 9 and Table 5 reveals that the working fluids in this region include R245fa and modern refrigerants and their mixtures. Modern refrigerants are characterized by very low GWP and zero flammability. For example, Novec 649 is therefore an interesting working fluid because of its low GWP and non-flammability. A power plant adopting the split-cycle configuration and Novec 649 as the working fluid entails a calculated  $\eta_{\text{cc}}$  higher than that of the benchmark, a  $VR$  of 23.6 and  $\Delta h_{\text{turbine}}$  of 32.7 kJ/kg. Such a fluid would fulfill regulations concerning environmental and operational safety and would allow the design of a compact and cost-effective turbine.

## 5. Conclusion

The use of mixtures as working fluids for air-cooled ORC systems as bottoming cycle of medium capacity gas turbines is investigated by means of steady state simulations. Zeotropic mixtures undergo isobaric phase change with a temperature glide, and this effect can in principle be exploited to reduce condenser fan power consumption at the cost of additional heat transfer surface. As a result, overall combined cycle efficiency may increase. Low GWP and non-flammable fluids suitable for high temperature waste heat recovery were considered. Furthermore, a new cycle configuration especially suitable for waste heat recovery was tested as a part of this study. The main findings are:

- In comparison to pure fluids, a larger number of mixtures can be used as working fluids of high-performance air-cooled ORC systems. However, in the case of the recuperated cycle configuration, even if the benefit of air-cooler fan power reduction is verified, under the given assumptions the performance of the benchmark case employing cyclopentane as the working fluid cannot be overcome, due to the higher exergy losses associated with heat transfer.
- The split-cycle configuration allows to increase the combined cycle efficiency if compared to the recuperated cycle configuration and the performance estimated with a wide range of working fluids is better than the performance calculated for the benchmark. The optimum combined cycle performance is achieved with pure fluids and mixtures featuring lower critical temperature as compared with the working fluids of the recuperated cycle configuration.
- A range of pure fluids and mixtures with lower critical temperatures may allow obtaining a conversion efficiency similar to that of the benchmark case but the resulting turbine is more compact and thus more cost-effective.
- The combined cycle efficiency of a system adopting the split-cycle configuration for the bottoming unit and Novec 649 as the working fluid, a low GWP and non-flammable fluid, is higher than the efficiency computed for the benchmark case.
- The adoption of mixtures as working fluid does not lead to a relevant performance increase with respect to the benchmark also if the condensation pressure is sub-atmospheric.

The performance improvement achieved with the split-cycle configuration comes at the cost of larger heat exchanger surfaces. In order to quantify the advantage of this configuration, the economic aspects related to the need of more heat transfer surface and to the turbine

design need to be taken into account. As a last remark, it must be noted that, while the PCP-SAFT equation of state employed in this study to calculate the thermodynamic properties of fluids belongs to the class of physics-based models, its application to highly non-ideal mixtures without a proper estimation of binary interaction parameters introduces some uncertainty.

### Declaration of competing interest

The authors declare that they have no known competing financial interests or personal relationships that could have appeared to influence the work reported in this paper.

### Data availability

Data will be made available on request.

### Acknowledgments

This research has been supported by the Applied and Engineering Sciences Division (TTW) of the Dutch Organization for Scientific Research (NWO), Open Technology Program of the Ministry of Economic Affairs, Grant No. 17906.

### References

- G. Bianchi, G.P. Panayiotou, L. Aresti, S.A. Kalogirou, G.A. Florides, K. Tsamos, S.A. Tassou, P. Christodoulides, Estimating the waste heat recovery in the European union industry, *Energy Ecol. Environ.* 4 (2019) 211–221.
- M. Papapetrou, G. Kosmadakis, A. Cipollina, U.L. Commare, G. Micale, Industrial waste heat: Estimation of the technically available resource in the EU per industrial sector, temperature level and country, *Appl. Therm. Eng.* 138 (2018) 207–216.
- P. Colonna, M. Astolfi, J. van Buijtenen, C. Wieland, G. David, F. Garofalo, M. Baresi, H. Öhman, W. Klink, Thermal Energy Harvesting: The Path to Tapping into a Large CO<sub>2</sub>-free European Power Source, Techreport, Knowledge Center on Organic Rankine Cycle technology, 2021, URL: [https://kcorc.org/media/medialibrary/2022/05/Thermal\\_Energy\\_Harvesting\\_-\\_the\\_Path\\_to\\_Tapping\\_into\\_a\\_Large\\_CO2-free\\_European\\_Power\\_Source.pdf](https://kcorc.org/media/medialibrary/2022/05/Thermal_Energy_Harvesting_-_the_Path_to_Tapping_into_a_Large_CO2-free_European_Power_Source.pdf).
- P. Colonna, E. Casati, C. Trapp, T. Mathijssen, J. Larjola, T. Turunen-Saaresti, A. Uusitalo, Organic rankine cycle power systems: From the concept to current technology, applications, and an outlook to the future, *J. Eng. Gas Turbines Power* 137 (2015).
- European Parliament, Directive 2014/34/EU of the European Parliament and of the Council of 26 February 2014 on the harmonisation of the laws of the member states relating to equipment and protective systems intended for use in potentially explosive atmospheres, 2014.
- European Parliament, Regulation (EU) no 517/2014 of the European Parliament and of the council of 16 April 2014 on fluorinated greenhouse gases and repealing regulation (EC) no 842/2006, 2014.
- G. Angelino, P. Colonna, Multicomponent working fluids for organic rankine cycles (ORCs), *Energy* 23 (6) (1998) 449–463.
- G. Angelino, P. Colonna, Air cooled siloxane bottoming cycle for molten carbonate fuel cells, in: *Fuel Cell Seminar*, Portland, OR, Oct. 30–Nov. 2, 2000, pp. 667–670.
- G. Angelino, P. Colonna, Organic rankine cycles for energy recovery from molten carbonate fuel cells, in: *35<sup>th</sup> Intersociety Energy Conversion Engineering Conference*, No. 2000–3052, IECEC, AIAA, 2000, pp. 1–11.
- K. Braimakis, A. Mikelis, A. Charalampidis, S. Karellas, Exergetic performance of CO<sub>2</sub> and ultra-low GWP refrigerant mixtures as working fluids in ORC for waste heat recovery, *Energy* 203 (2020) 117801.
- G.B. Abadi, K.C. Kim, Investigation of organic rankine cycles with zeotropic mixtures as a working fluid: Advantages and issues, *Renew. Sustain. Energy Rev.* 73 (2017) 1000–1013.
- Y. Fang, F. Yang, H. Zhang, Comparative analysis and multi-objective optimization of organic rankine cycle (ORC) using pure working fluids and their zeotropic mixtures for diesel engine waste heat recovery, *Appl. Therm. Eng.* 157 (2019) 113704.
- M. Kolahi, M. Yari, S. Mahmoudi, F. Mohammadkhani, Thermodynamic and economic performance improvement of ORCs through using zeotropic mixtures: Case of waste heat recovery in an offshore platform, *Case Stud. Therm. Eng.* 8 (2016) 51–70.
- R. Scaccabarozzi, M. Tavano, C.M. Invernizzi, E. Martelli, Comparison of working fluids and cycle optimization for heat recovery ORCs from large internal combustion engines, *Energy* 158 (2018) 396–416.
- Z. Ge, J. Li, Q. Liu, Y. Duan, Z. Yang, Thermodynamic analysis of dual-loop organic rankine cycle using zeotropic mixtures for internal combustion engine waste heat recovery, *Energy Convers. Manage.* 166 (2018) 201–214.
- L.-H. Zhi, P. Hu, L.-X. Chen, G. Zhao, Parametric analysis and optimization of transcritical-subcritical dual-loop organic rankine cycle using zeotropic mixtures for engine waste heat recovery, *Energy Convers. Manage.* 195 (2019) 770–787.
- G. Di Marcoberardino, C. Invernizzi, P. Iora, A. Ayub, D. Di Bona, P. Chiesa, M. Binotti, G. Manzolini, Experimental and analytical procedure for the characterization of innovative working fluids for power plants applications, *Appl. Therm. Eng.* 178 (2020) 115513.
- Y. Yang, T. Xue, Z. Rao, S. Liao, Potential of transcritical recompression rankine cycle operating with CO<sub>2</sub>-based binary mixtures, *Energy Convers. Manage.* 252 (2022) 115040.
- F. Crespi, P.R. de Arriba, D. Sánchez, A. Ayub, G. Di Marcoberardino, C.M. Invernizzi, G. Martínez, P. Iora, D. Di Bona, M. Binotti, et al., Thermal efficiency gains enabled by using CO<sub>2</sub> mixtures in supercritical power cycles, *Energy* 238 (2022) 121899.
- J. Ren, Y. Cao, Y. Long, X. Qiang, Y. Dai, Thermodynamic comparison of gas turbine and ORC combined cycle with pure and mixture working fluids, *J. Energy Eng.* 145 (1) (2019) 05018002.
- A.I. Papadopoulos, M. Stijepovic, P. Linke, P. Seferlis, S. Voutetakis, Molecular design of working fluid mixtures for organic rankine cycles, *Comput. Aided Chem. Eng.* 32 (2013) 289–294.
- J. Schilling, M. Entrup, M. Hopp, J. Gross, A. Bardow, Towards optimal mixtures of working fluids: Integrated design of processes and mixtures for organic rankine cycles, *Renew. Sustain. Energy Rev.* 135 (2021) 110179.
- J. Gross, J. Vrabec, An equation-of-state contribution for polar components: Dipolar molecules, *AIChE J.* 52 (3) (2006) 1194–1204.
- M. Gaia, R. Bini, R. Vescovo, E. Spagnoli, Cogenerative Organic Rankine Cycle System, Patent WO2017199170A1, World Intellectual Property Organization, 2017.
- W. Klink, Personal communication with Wolfgang Klink of Siemens Energy AG, 2018.
- R. Rowley, W. Widling, J. Oscarson, Y. Yang, N. Zundel, T. Daubert, R. Danner, DIPPR® Data Compilation of Pure Chemical Properties, Design Institute for Physical Properties, AIChE, New York, NY, USA, 2006.
- L. Calderazzi, P. Colonna, Thermal stability of R-134a, R-141b, R-131i, R-7146, R-125 associated with stainless steel as a containing material, *Int. J. Refrig.* 20 (1997) 381–389.
- M. Astolfi, E. Macchi, Organic Rankine Cycle (ORC) Power Systems, Elsevier, 2017.
- C. Arpagaus, F. Bless, M. Uhlmann, J. Schiffmann, S.S. Bertsch, High temperature heat pumps: Market overview, state of the art, research status, refrigerants, and application potentials, *Energy* 152 (2018) 985–1010.
- K. Kontomaris, HFO-1336mzz-Z: High Temperature Chemical Stability and Use as a Working Fluid in Organic Rankine Cycles, Purdue University, 2014.
- C. Mateu-Royo, J.N.-E.A. Mota-Babiloni, M. Amat-Albuixech, F. Molés, Thermodynamic analysis of low GWP alternatives to HFC-245fa in high-temperature heat pumps: HCFO-1224yd(Z), HCFO-1233zd(E) and HFO-1336mzz(Z), *Appl. Therm. Eng.* 152 (2019) 762–777.
- J.R. Juhasz, Novel working fluid, HFO-1336mzz(E), for use in waste heat recovery application, in: *12th IEA Heat Pump Conference*, 2017.
- M.O. McLinden, A.F. Kazakov, J.S. Brown, P.A. Domanski, A thermodynamic analysis of refrigerants: Possibilities and tradeoffs for low-GWP refrigerants, *Int. J. Refrig.* 38 (2014) 80–92.
- 3M Corporation, Novec™ 649 product datasheet, 2009, URL: <https://multimedia.3m.com/mws/media/5698650/3m-novec-engineered-fluid-649.pdf>.
- K. Takizawa, K. Tokuhashi, S. Kondo, Flammability assessment of CH<sub>2</sub>CF<sub>3</sub>: Comparison with fluoroalkenes and fluoroalkanes, *J. Hazard. Mater.* 172 (2009) 1329–1338.
- R.A. Perkins, M.L. Huber, M.J. Assael, Measurement and correlation of the thermal conductivity of trans-1-Chloro-3,3,3-trifluoropropene (R1233zd(E)), *J. Chem. Eng. Data* 62 (2017) 2659–2665.
- F2 Chemicals Ltd., FLUTECH® Product Datasheet, F2 Chemicals Ltd., 2012, URL: <https://f2chemicals.com/pdf/technical/Compatibility.pdf>.
- K.N. Marsh, A. Abramson, D. Ambrose, D.W. Morton, E. Nikitin, C. Tsonopoulos, C.L. Young, Vapor-liquid critical properties of elements and compounds. 10. Organic compounds containing halogens, *J. Chem. Eng. Data* 52 (2007) 1509–1538.
- M.O. McLinden, R.A. Perkins, E.W. Lemmon, T.J. Fortin, Thermodynamic properties of 1,1,1,2,2,4,5,5,5-nonfluoro-4-(trifluoromethyl)-3-pentanone: Vapor pressure, (p, ρ, T) behavior, and speed of sound measurements, and an equation of state, *J. Chem. Eng. Data* 60 (2015) 3646–3659.
- W.J. Collins, R.G. Derwent, C.E. Johnson, D.S. Stevenson, The oxidation of organic compounds in the troposphere and their global warming potentials, *Clim. Chang.* 52 (2002) 453–479.
- IPCC, Climate Change 2013: The Physical Science Basis. Contribution of Working Group I to the Fifth Assessment Report of the Intergovernmental Panel on Climate Change, Cambridge, United Kingdom and New York, NY, USA, 2013.

- [42] X. Dai, L. Shi, Q. An, W. Qian, Screening of hydrocarbons as supercritical ORCs working fluids by thermal stability, *Energy Convers. Manage.* 126 (2016) 632–637.
- [43] M. Preißinger, D. Brüggemann, Thermal stability of hexamethyldisiloxane (MM) for high-temperature organic rankine cycle (ORC), *Energies* 9 (2016) 183.
- [44] G. Angelino, C. Invernizzi, Experimental investigation on the thermal stability of some new zero ODP refrigerants, *Int. J. Refrig.* 26 (2003) 51–58.
- [45] P. Colonna, T. van der Stelt, FluidProp (Version 3.1): A program for the estimation of thermophysical properties of fluids, 2019.
- [46] J. Gross, G. Sadowski, Perturbed-chain SAFT: An equation of state based on a perturbation theory for chain molecules, *Ind. Eng. Chem. Res.* 40 (4) (2001) 1244–1260.
- [47] P. Rehner, A. Bardow, J. Gross, Modeling mixtures with PC-SAFT: Insights from large-scale parametrization and group-contribution method for binary interaction parameters, *J. Thermophys.* (2023) Preprint.
- [48] J. Liu, Y. Liu, C. Liu, L. Xin, W. Yu, Experimental and theoretical study on thermal stability of mixture R1234ze (E)/R32 in organic rankine cycle, *J. Therm. Sci.* (2023) 1–19.
- [49] S. Gallarini, A. Spinelli, L. Lietti, A. Guardone, Thermal stability of linear siloxanes and their mixtures, *Energy* 278 (2023) 127687.
- [50] F.-A. Fortin, U.M.-A. Gardner, M. Parizeau, C. Gagné, DEAP: Evolutionary algorithms made easy, *J. Mach. Learn. Res.* 13 (2012) 2171–2175.
- [51] G. Angelino, C. Invernizzi, E. Macchi, Organic working fluid optimization for space power cycles, *Mod. Res. Top. Aerosp. Propuls.* (1991) 297–326.